

A search for non-random cosmic-ray time series by a cluster analysis^(*)

Y. KATAYOSE, Y. INOUE, Y. KAWASAKI, H. MIYOSHI, S. MURAKAMI
M. NAKAGAWA, T. NAKAKOJI, E. NAKANO, T. TAKAHASHI and Y. TERAMOTO

*Institute for Cosmic Ray Physics, Osaka City University
3-3-138 Sugimoto, Sumiyoshi-ku, Osaka 558, Japan*

(ricevuto il 21 Maggio 1997; revisionato il 26 Gennaio 1998; approvato il 3 Marzo 1998)

Summary. — Non-random time series of cosmic rays were searched for in air shower data of mean energy 1.1×10^{15} eV, collected by the air shower array at Mitsuishi, Japan, during the period from January 1989 to October 1996. By clustering the arrival time of air showers, five occasions of rate elevation phenomena were found with an expected probability ≤ 0.05 (varying from 0.18×10^{-2} to 4.0×10^{-2}) from a random distribution in 3651358 air showers. The arrival directions of these events are grouped in two regions on the galactic plane within the latitude $\pm 25^\circ$, corresponding to a chance probability of 1.6% from a uniform distribution.

PACS 98.70.Sa – Cosmic rays (including sources, origin, acceleration, and interactions).
PACS 96.40.Pq – Extensive air showers.

1. – Introduction

Although high-energy cosmic rays are generally assumed to arrive at the Earth randomly, some evidence for non-randomness has been reported by several groups. Bhat *et al.* [1] have reported the possible existence of non-random components in air showers with energies $\geq 10^{14}$ eV. If the arrival time of the high-energy primary cosmic ray is random, the arrival time of the air shower, initiated by the primary cosmic ray, should also be random. In this case, the distribution of arrival time intervals for air showers should fall off exponentially with a time constant that is the reciprocal of the air shower rate. Bhat *et al.*, however, observed two exponential components in the distribution with a kink at roughly 40 s. When the events with time intervals less than 40 s were mapped to the areas in the sky, a peak was observed at right ascension (5 ± 3) h.

Further evidence to support this result has been reported by Badino *et al.* [2]. They measured the muon rate deep underground and found evidence for an event rate excess in

(*) The authors of this paper have agreed to not receive the proofs for correction.

the time interval (< 40 s), similar to Bhat *et al.* On the other hand, negative results have been reported by several other groups [3, 4]. Fegan *et al.* used a ground level air shower array to search for the Bhat-type anomaly in 20 000 showers with energies $\geq 10^{14}$ eV and 5000 showers with energies $\geq 10^{15}$ eV. Their result was negative.

Although the measurements of Bhat *et al.* and Badino *et al.* concern the non-randomness in long-term phenomena, evidences for short-term non-random phenomena have also been reported. Smith *et al.* [5] reported a burst event with distinct structure in its time series. They observed a random temporal sequence of 32 air showers, of mean energy 3×10^{15} eV, within a 5 min time interval at one station at Winning, Canada, on January 20, 1981. There was no other burst observed in the experiment which sampled 150 000 shower triggers over the 18 month period. Another incident has been reported by Fegan *et al.* [6]. They observed a single incidence of simultaneous increase in the air shower rates at two recording stations separated by 250 km during three years of observation. The event lasted for 20 s. Furthermore, Kitamura *et al.* [7] reported on a chaotic feature in the time series of the arrival times of air showers with energies $> 3 \times 10^{14}$ eV. Although arrival time intervals of over 99.9% of the air showers obeyed a Poisson distribution, representing stochastic behavior, they observed 13 events that show chaotic behavior as opposed to either random or colored noise. For five events among the ten chaotic events, we also found chaotic behavior in the Mitsubishi data in the time period which overlapped with their events [8]. It should be noted that the Mitsubishi air shower array is located 115 km from the Kinki University's air shower array. One possible explanation for these chaotic events is that they originate from energetic cosmic-ray dust particles.

In this article, we report the results of a search for non-random time series (clustered events) in air shower arrival times. These phenomena are characterized by an elevated event rate with a duration of the order of minutes to hours, having arrival time intervals of the order of less than one to several minutes. The data used were collected using the Mitsubishi air shower array during the period from January 1989 to October 1996, corresponding to 2427 days. The arrival time intervals of air showers were analyzed by a cluster method, which is particularly sensitive to searches for clustered events with long durations. Five events were found with a high significance of non-randomness. The arrival directions of the events are grouped on the galactic plane.

2. – Detector and data taking

The Mitsubishi air shower array is located at Mitsubishi, Japan (latitude 34.8°N , longitude 134.3°E) at an altitude of 130 m. It has been continuously operated since its first operation in 1961. The air shower array consists of 16 scintillation counters and an underground muon detector (figs. 1, 2). The scintillation counters are placed at ground level, covering roughly $40 \times 50 \text{ m}^2$. The size of each scintillator is $100 \text{ (W)} \times 100 \text{ (L)} \times 10 \text{ (H)} \text{ cm}^3$, viewed by a 5 inch photomultiplier tube.

The muon detector is made of four layers of proportional chambers; two layers in x and two layers in y , as shown in fig. 3. The x -directional layer consists of 26 rectangular tube-type counters, $10 \times 5 \times 450 \text{ cm}^3$, making the total effective area $260 \times 450 \text{ cm}^2$, with 5 cm cell size. Each counter has two sensing wires; each sensing wire is connected to an individual readout channel. The y -directional layer consists of 4 planar chambers, $122 \times 5 \times 239 \text{ cm}^3$, making the total effective area $440 \times 239 \text{ cm}^2$, with 10 cm cell size. Each chamber has 22 sensing wires and each pair of adjacent wires are connected together before connecting to each readout channel [9]. The muon detector is located

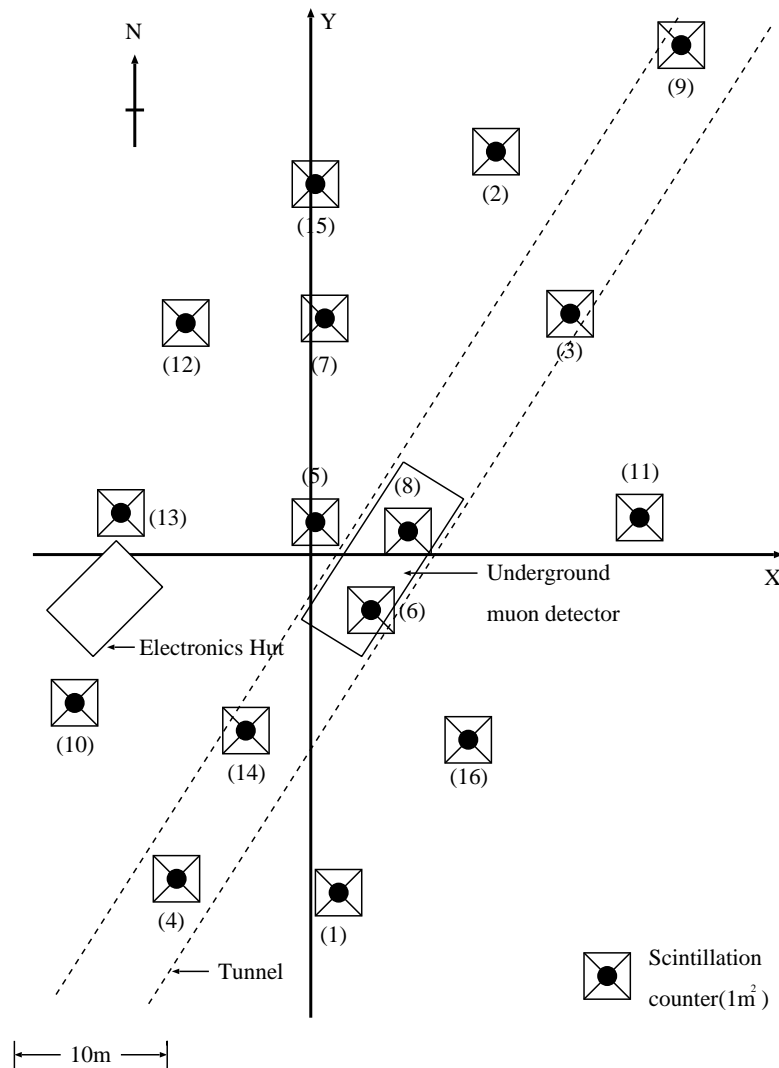


Fig. 1. - Top view of the Mitsubishi air shower detector. The air shower array consists of 16 scintillation counters on the ground. The muon detector consists of four layers of proportional chambers placed in the tunnel at 30 m.w.e. depth under the surface.

in the tunnel at 30 m.w.e. depth, approximately under the center of the surface array, requiring a minimum muon momentum $P_\mu > 6$ GeV to penetrate into the detector.

The two detector systems, the surface array and the underground muon detector, are electrically isolated. This isolation reduces the chances of having accidental pickup of common electrical noise. The trigger requires a coincidence between hits in the three scintillators in the central region (counters 5, 6, 8 in fig. 1) and hits in the two x -directional layers of the muon chambers (fig. 4(a)). After a trigger, each analog signal is converted into digital and recored by a personal computer, as shown in fig. 4(b). This trigger condition requires the core position of air showers to be near to the center of the array.

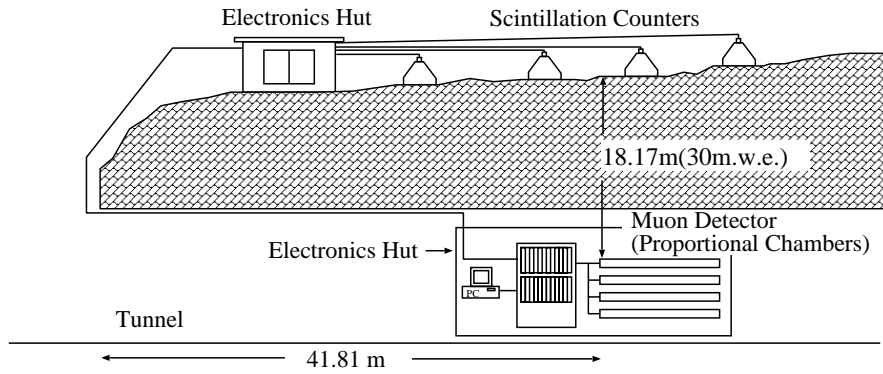


Fig. 2. - Schematical side view of the Mitsubishi air shower detector.

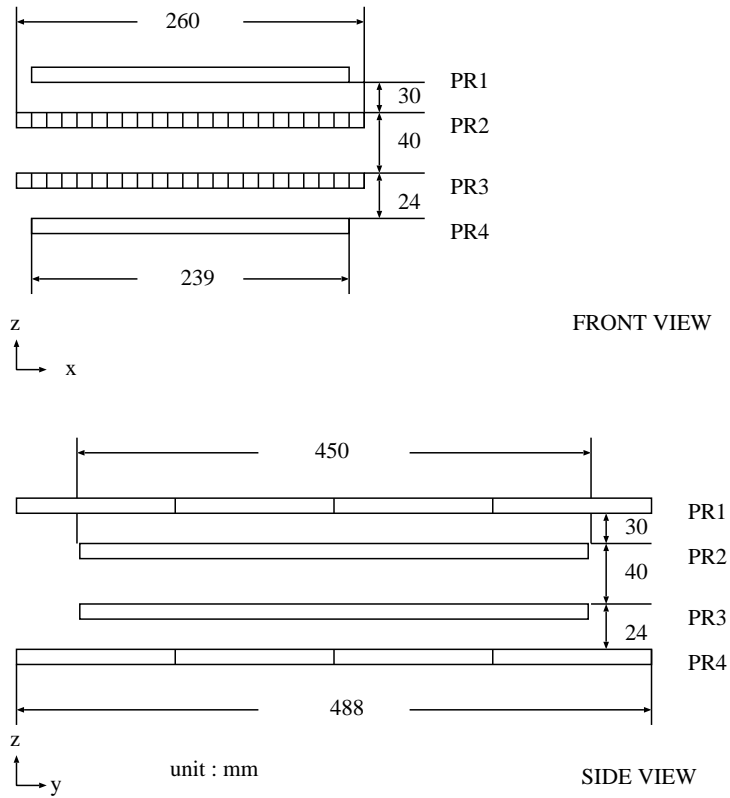


Fig. 3. - The muon detector made of four layers of proportional chambers. The solid-angle area of the detector is $19.1 \text{ m}^2 \text{ sr}$. The accuracy of zenith angle determination is $\pm 3^\circ$ for muons.

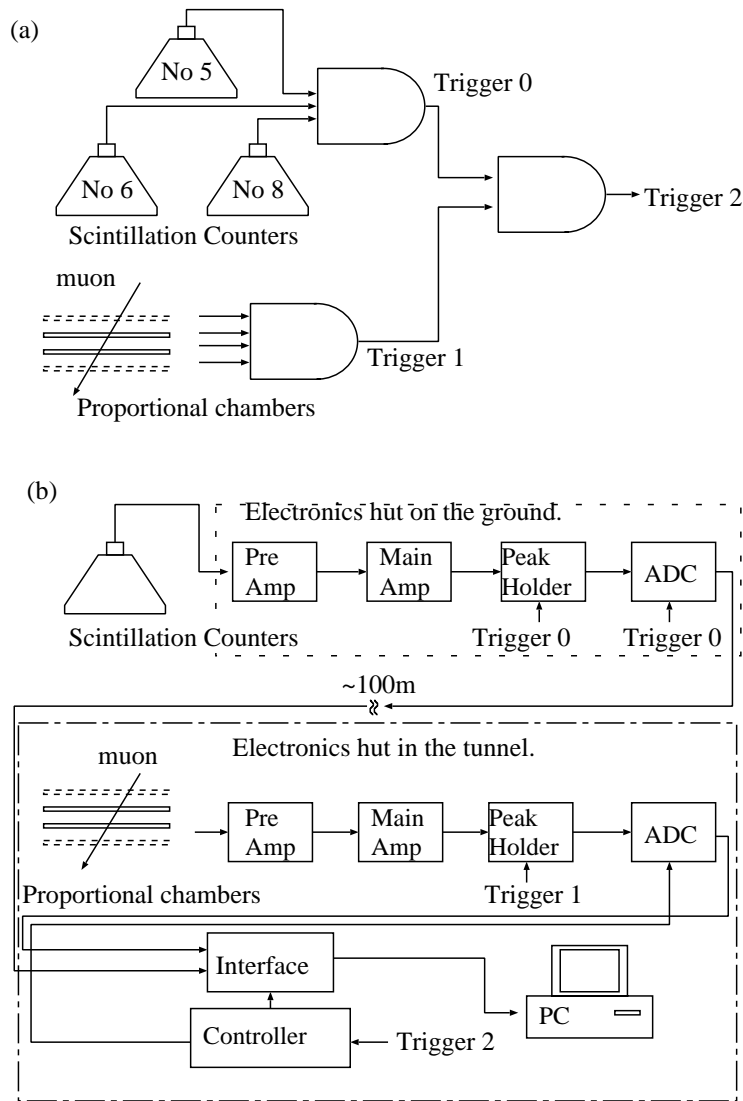


Fig. 4. - The data taking system of the Mitsubishi air shower detector. (a) Trigger logic. Data were recorded when three scintillators in the center region of the array and two x -directional layers of muon chambers were fired simultaneously. (b) Block diagram of the data taking system.

3. - Data analysis and results

In this analysis, the data from January 1989 to October 1996 were used. The total observation time was 2427 days. The trigger rate was approximately 1 event/min. In the first step of the analysis, event selection was made by imposing two conditions: 1) all the layers of the muon chambers have hits, 2) ≥ 5 scintillators have hits. More than 85% of the recorded data passed these conditions. Air showers were reconstructed for these events. Directions of air showers were determined by the muon directions in the

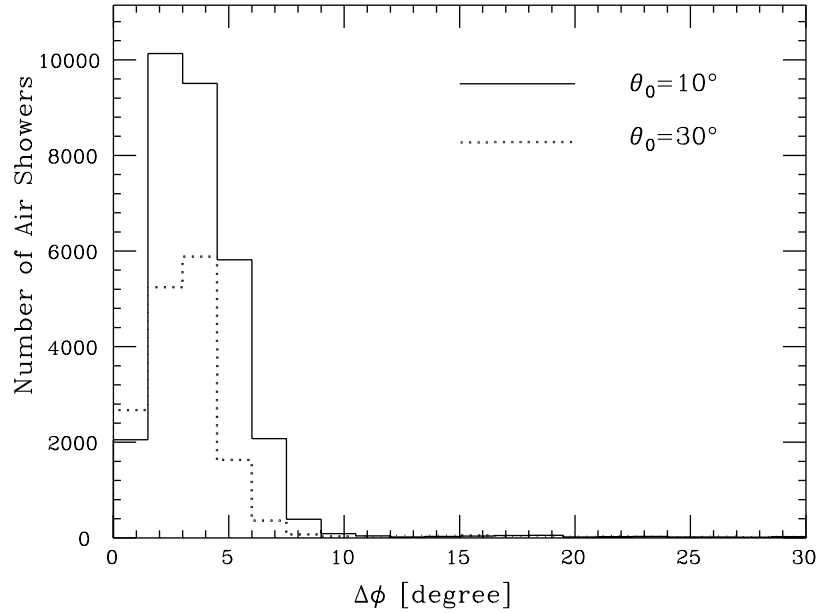


Fig. 5. – Comparison of the measured and the original air shower directions by MC at two zenith angles ($\theta_0 = 10^\circ$ and $\theta_0 = 30^\circ$). The air shower simulation was done by Cosmos.uv4.00. The opening angle, $\Delta\phi$ between the measured and the original air shower directions are shown by the solid line for $\theta_0 = 10^\circ$ and dotted line for $\theta_0 = 30^\circ$. The mean differences are 4.0° for $\theta_0 = 10^\circ$ and 4.3° for $\theta_0 = 30^\circ$, respectively.

air showers. Previous studies [10], using Monte Carlo simulations, have shown that the average difference between the air shower direction and the average muon direction is less than 1° for $P \geq 6$ GeV muons.

The muon direction was determined by fitting to the hits in the proportional chambers. Fits were done separately in X view and Y view. In each view, straight lines were drawn by fitting to the hits in the two layers of the muon chambers. If there was only one line, we accepted the direction of the line as the muon direction. If there were more than one line and if there were parallel lines among them, the direction of the parallel lines was accepted as the muon direction. If there were more than one set of parallel lines, the direction of the set with the largest numbers of parallel lines was accepted as the muon direction. If there were more than one set of parallel lines with equal largest numbers of parallel lines, the average direction of the sets was accepted as the muon direction. If there was no parallel line, we selected the direction of the line with smaller (projected) zenith angle as the muon direction.

After the muon direction of each view was determined, we obtained the 3D direction by combining the directions of X and Y views. The accuracy of this method was studied by Monte Carlo [11]. Figure 5 shows the difference between the measured and original air shower directions. The average angular resolution for the air showers is 3.8° for a zenith angle of less than 45° . Air shower parameters, size N_e and core location, were determined by a least-square fit of the observed particle density to an NKG lateral distribution. 99% of the data passed the air shower analysis. The measured air shower size distribution is shown in fig. 6. The mean air shower size was $N_e = 1.4 \times 10^5$, which corresponds to a

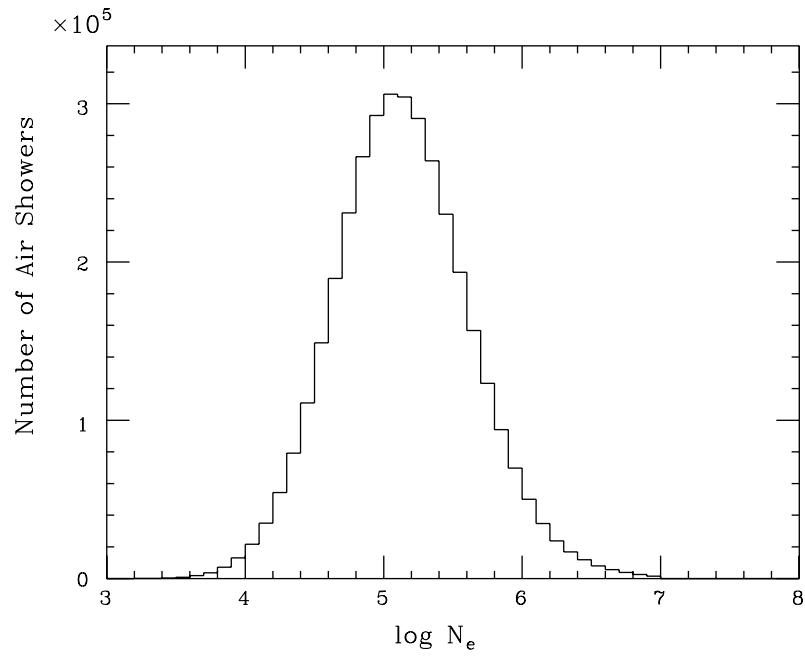


Fig. 6. - Size distribution of air showers. The mean air shower size was $N_e = 1.4 \times 10^5$.

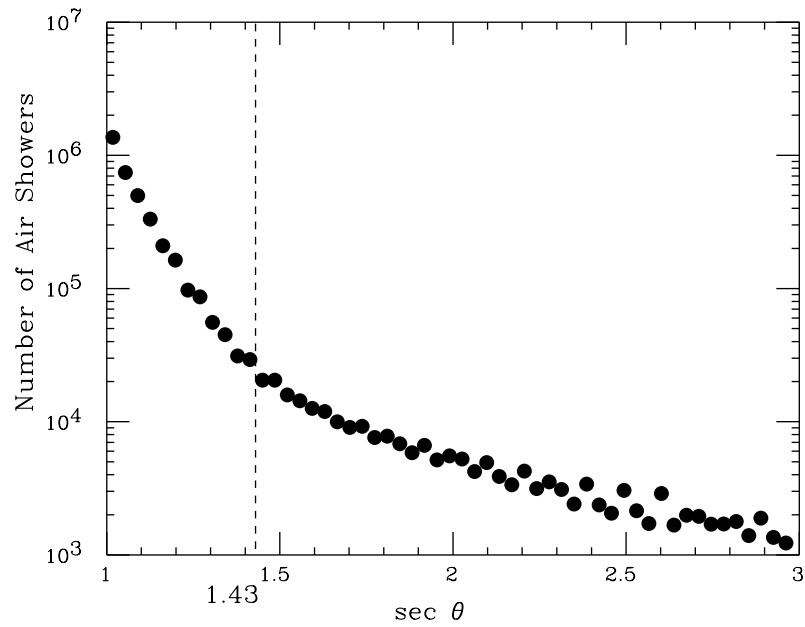


Fig. 7. - Zenith angle distribution. The distribution has a sharp peak at the vertical direction. The events with zenith angles smaller than 45° ($\sec \theta = 1.43$) were used for the cluster analysis.

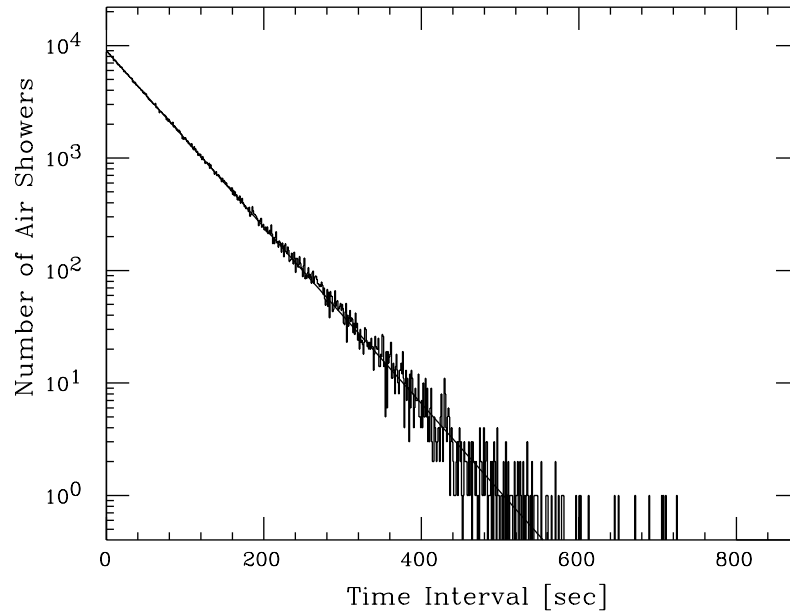


Fig. 8. – Arrival time intervals of the air showers in the 1995 data. The line shows the fit to the data using the $N = N_0 \exp[-\lambda t]$ form, where $N_0 = N^2/T$, $\lambda = N/T$.

primary energy of 1.1×10^{15} eV. The zenith angle distribution of the observed air showers is shown in fig. 7. The distribution has a peak at the vertical direction, which falls off exponentially to 45° as a function of $\sec \theta$. We accepted air showers with zenith angles $\leq 45^\circ$ for further analysis. After this selection, 3651358 events remained. A cluster method was applied to these events.

If the arrival time of cosmic rays is random, the event rate will follow a Poisson distribution, in which case the arrival time interval between successive air showers follows an exponential law. Figure 8 shows the arrival time intervals of air showers. The distribution follows the exponential form: $n = (N^2/T) \exp[-Nt/T]$, where N is the total number of events and T is the total period of time. Figure 9 shows the number of air showers in 20 minute time bins. The result is consistent with a Poisson process and no anomaly was found in this distribution. This method, however, is insensitive to burst-like increases of event rate, which may occur a few times in a year. A burst-like (clustered) event is characterized by its start time and its duration; those are free parameters and should be determined by the analysis. Buccheri *et al.* [12, 13] introduced a cluster method for finding such events. In their method, the events are grouped into clusters when the time interval, Δt , between consecutive events is shorter than a given value, t_α , as shown in fig. 10. The cluster is then terminated by an event with $\Delta t > t_\alpha$.

In our analysis, the eight years of data were divided into groups of events in several month periods with approximately constant event rate. Clustered events were separately searched for in each group and the results were combined at the end. Figure 11(a) shows the distribution of arrival time intervals in the data taken from 19th September to 14th October 1990. The dip at $\Delta t < 3$ s is caused by the dead time of the system. To correct the effect of dead time, we selected the events which were observed 3 s or more than 3 s after each selected event. Then 3 s were subtracted from the time interval of each

remained event after this selection. After this correction, the distribution is exponential, as shown in fig. 11(b). We adapted Buccheri's method for grouping events into clusters. We used $t_\alpha = 5, 10, 15, 20, 25$ (s) for $t_\alpha < 30$ s, and for $30 \leq t_\alpha \leq 400$ (s), t_α was increased in steps of 10 s.

In Buccheri's method, the probability of chance occurrence for each clustered event is calculated as a function of the number of events in each cluster with a duration time, t , as

$$(1) \quad P(x \geq n, t) = 1 - \exp[-Nt/T] \sum_{i=0}^{n-1} \frac{(Nt/T)^{n-i-1}}{(n-i-1)!},$$

where n is the number of events in t , N is the total number of events in the total period of time, T . This method is sensitive to clustered events with short duration time. We used a different formula to calculate the probability. The modified method has a better sensitivity to phenomena with a long duration of increased event rate, of the order of several hours.

In this method, we require "no break" of events in a cluster, *i.e.* every t_α time bin in the cluster has to have at least one event in it. When the elevation of event rate is small, the difference in probability for satisfying the "no break" condition is not significant between a time series with the elevated event rate and the normal level. However, by accumulating 10^2 to 10^3 events in a large cluster, the small difference of probability for each "no break" is also accumulated. Hence, in a large cluster, the background probability, due to the chance occurrence by normal rate events, can be greatly reduced. Because of this reduction of background probability in a large cluster, a small increase in event rate of long duration can be detected using this method. In other words, if cosmic rays are arriving randomly with a constant average rate, such large clusters should not exist. Evidence for

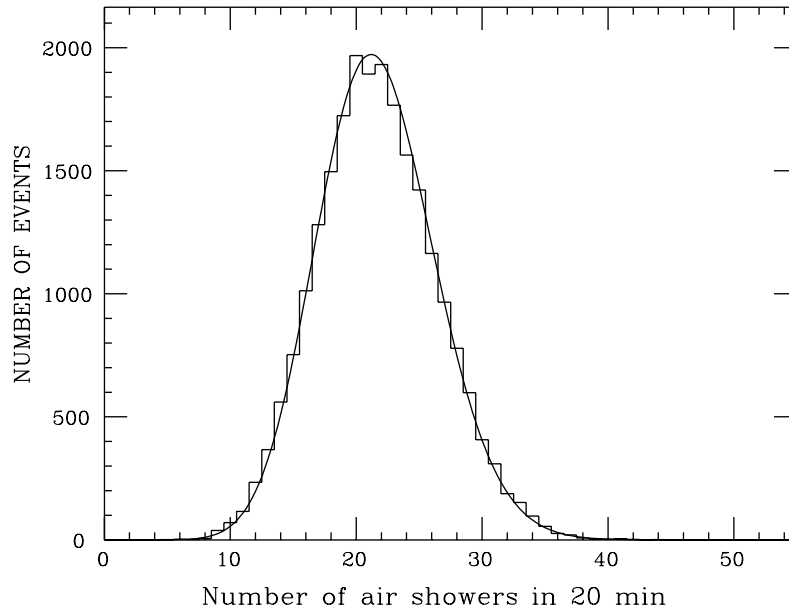


Fig. 9. – The distribution of the event rate every 20 minutes in the 1995 data. The data are shown by the histogram and the curve shows the fit by a Poisson distribution.

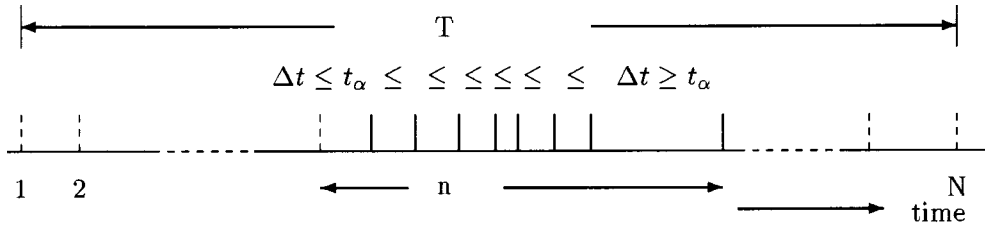


Fig. 10. – Illustration of the cluster method. Events are grouped into a cluster, when the first $n - 1$ consecutive pairs of events have time intervals smaller than a predefined value t_α and the last consecutive pair of events has a time interval larger than t_α . T is the total period of observation time and N is the total number of events in T .

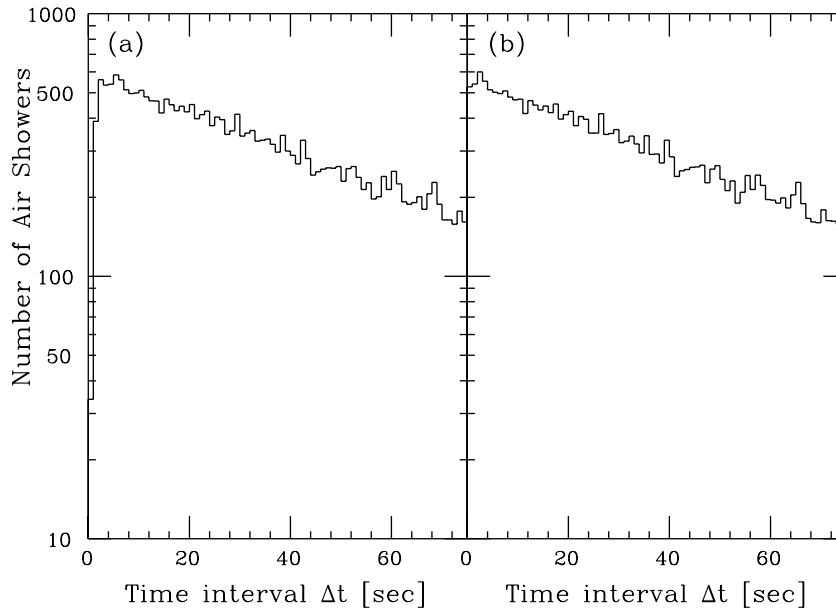


Fig. 11. – The time interval distribution of the data from 9/19 to 10/14 in 1990. (a) The distribution before removal of dead time. The dip in the region from 0 to 3 (s) is due to the dead time of the data taking system. (b) The distribution after removal of dead time. In order to correct the effect of dead time, the events, which arrived within 3 seconds after each selected event, were removed. Then 3 s was subtracted from the time interval of each remained event.

TABLE I. – Observed clustered events.

Date	Time (UT)	t_α (s)	t (s)	n	Expectation in 2427 days	RA (deg.)	Dec. (deg.)
890514	021552	300	117395	1346	1.8×10^{-3}	75	33
900929	172805	200	22005	398	4.0×10^{-2}	90	33
910214	210021	320	143837	2591	8.4×10^{-3}	47	33
940220	222405	150	9916	232	1.9×10^{-2}	281	33
940515	200429	60	1145	41	3.6×10^{-2}	310	34

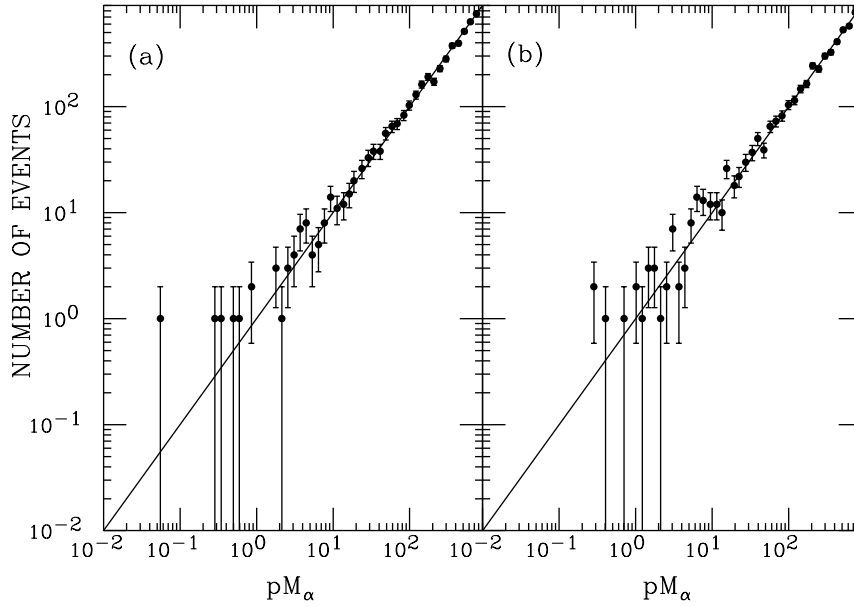


Fig. 12. – The number of clustered events vs. pM_α , where p was calculated by eq. (2). (a) Monte Carlo simulation and (b) observed data in 1995.

such clusters indicates that the cosmic-ray rate deviates from a random distribution with a constant average rate. It should be noted that it is crucial to choose the proper t_α for the elevated level to separate a cluster from background.

We searched for the possible existence of such large clusters in our air shower data. The expected probability of having a cluster in the total observation time, T , is given by pM_α , where M_α is the total number of observed clusters in T and p is the probability of chance occurrence of the cluster. The probability, p , is calculated from the arrival time interval distribution. In a Poisson process, the probability of having the next event within a time interval of t_α is $1 - \exp[-Nt_\alpha/T]$. Thus the probability of occurrence of a cluster with size n is

$$(2) \quad p(x = n) = (1 - \exp[-Nt_\alpha/T])^{n-1} \exp[-Nt_\alpha/T].$$

We verified this expression by applying this to both the Monte Carlo (MC) data and the observed data. Figure 12(a) shows the number of clusters found in the MC data as a function of pM_α , where p is calculated by eq. (2). The result is consistent with the calculation. Figure 12(b) shows the pM_α of the observed data with no significant clustered event. The observed distribution is also consistent with the calculation. To compare the data with expectation, the probability of having a cluster with a number of events equal to or greater than n was calculated, which is

$$(3) \quad P(x \geq n) = 1 - \sum_{i=1}^{n-1} (1 - \exp[-Nt_\alpha/T])^{i-1} \exp[-Nt_\alpha/T].$$

The probability of occurrence of each cluster for the total observation period T_0 (2427

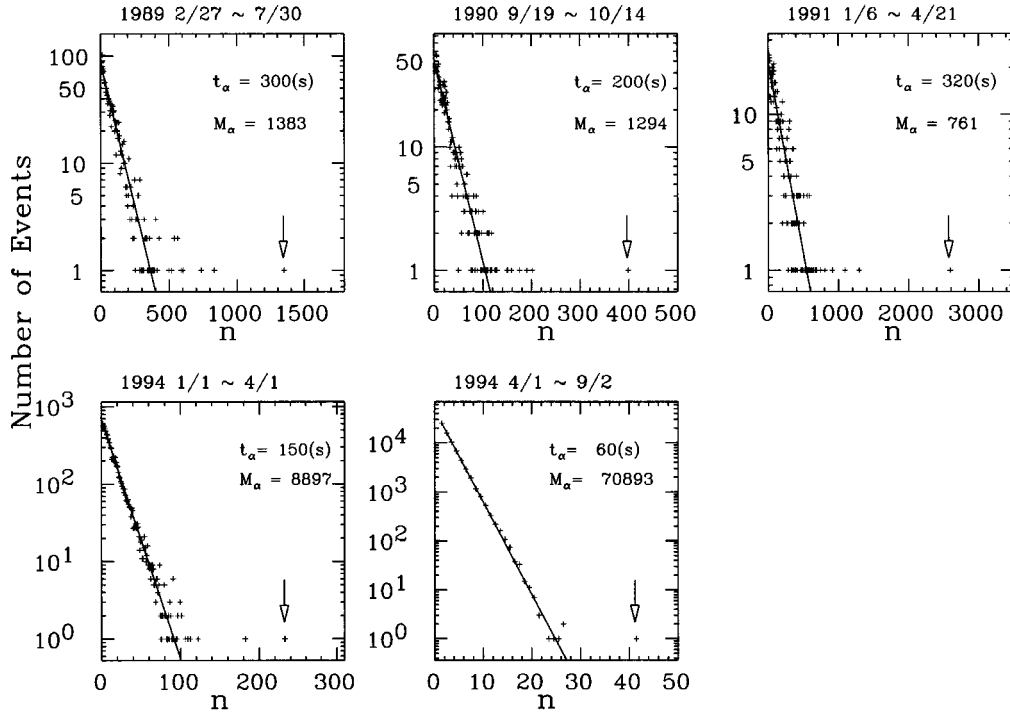


Fig. 13. – The number of consecutive events for the five clustered events; vertical crosses show the data and solid lines show the expectations derived from Poisson distribution. The clustered events are indicated by the arrows.

days) was calculated by $PM_\alpha T_0/T$. The event was considered as significant if $PM_\alpha T_0/T$ of the cluster was smaller than 0.05.

After this selection, we have found five significant clusters, which are listed in table I. In table I, the starting time of each cluster is shown in the format: date = yymmdd, time = hhmmss. The threshold time interval, t_α , of the five clusters varies from 60 to 320 (s). The number of air showers in each cluster varies from $n = 41$ in the shortest cluster ($t = 19.2$ min) to $n = 2591$ in the longest cluster ($t = 40.0$ hour). Figure 13 shows the number of events for each cluster with the t_α used. The expectation probability of each cluster from a uniform distribution varies from 0.18×10^{-2} to 4.0×10^{-2} for the total observation period. The size and the zenith angle distributions of the air showers in the clustered events are shown in figs. 14 and 15, respectively. No significant difference was found between the air showers in the clustered events and the normal air showers.

Arrival directions of the clustered events were studied by using the air shower directions in the clusters. Figure 16 shows the right ascension of the air showers in each clustered event. Each distribution has one or two peaks. Figure 17 shows the average direction of the air showers in the clustered event in the galactic coordinate system. The observable region for the Mitsubishi air shower array is $-10^\circ < \text{declination} < 80^\circ$, mainly due to the zenith angle cut at 45° . The dotted line shows the meridian at Mitsubishi. All of the five events are grouped around the line. The right ascension of the air showers in the clustered events has two peaks in its distribution, as shown in fig. 18. The obser-

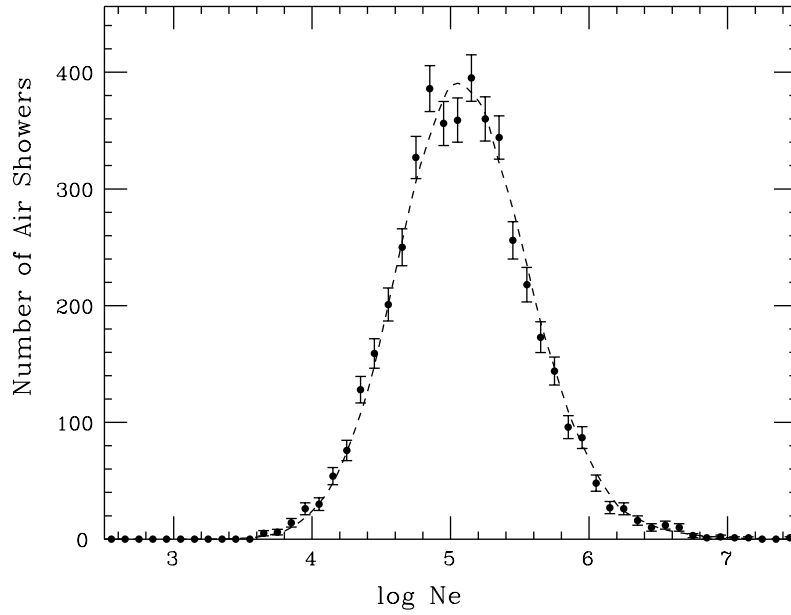


Fig. 14. - The air shower sizes in the clustered events. The clustered events are shown by the filled circles and the dashed curve shows the normal air showers.

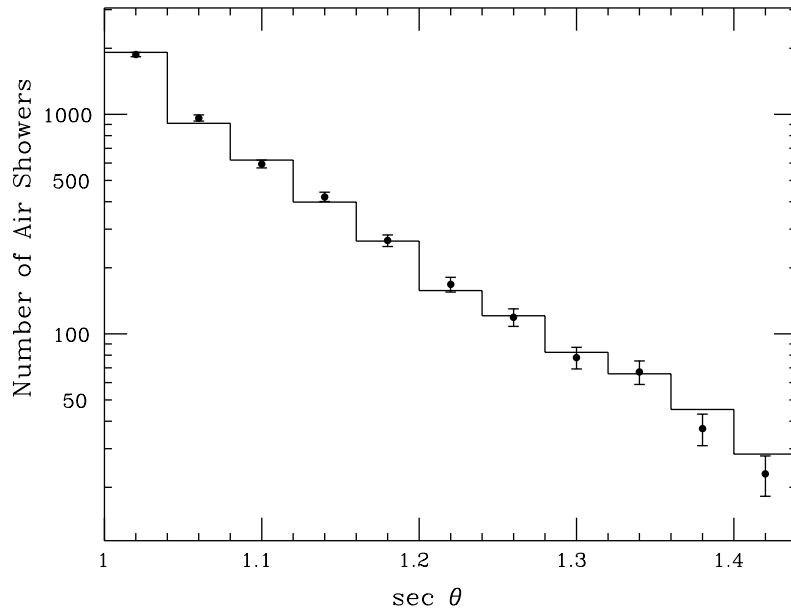


Fig. 15. - The zenith angles of the air showers in the clustered events. The clustered events are shown by the filled circles and the histogram shows the normal air showers.

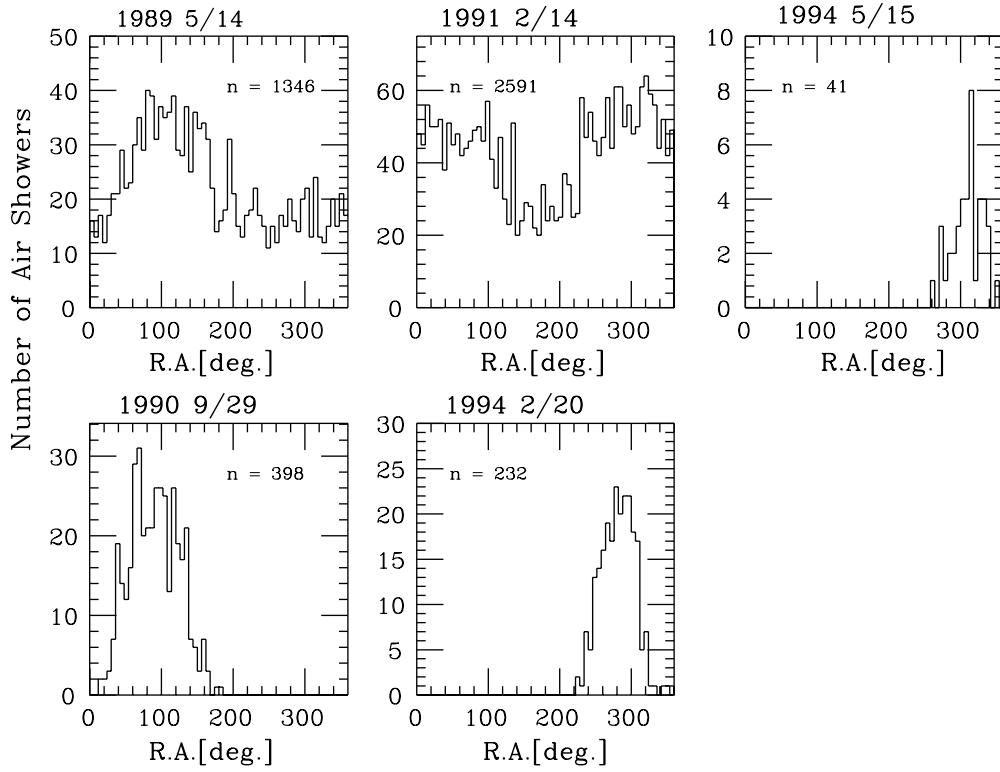


Fig. 16. - The right ascension (RA) of the air showers in the clustered events.

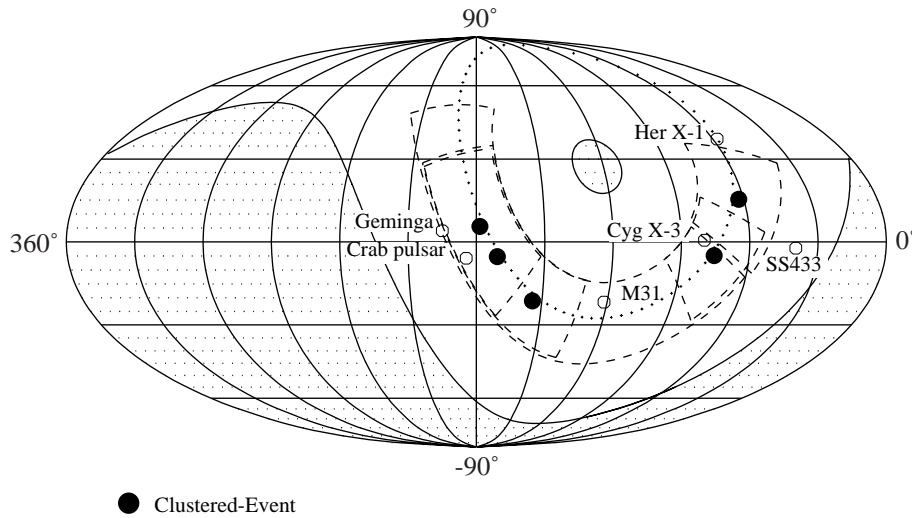


Fig. 17. - The directions of the clustered air showers. The average directions of the air showers in the five clustered events are shown in the galactic coordinate. The standard deviation of the average direction for each cluster is shown as a dashed box. The dotted line shows the meridian at Mitsuishi. The sky not observed by the Mitsuishi air shower array, due to the zenith angle cut at 45°, is shown as the hatched area.

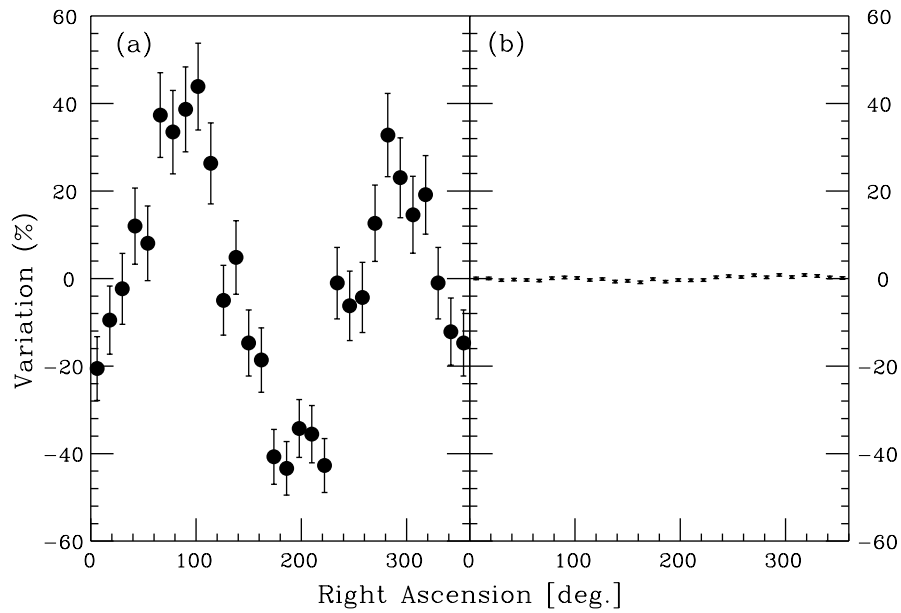


Fig. 18. - Variations of right ascension for (a) the air showers in the clustered events and (b) all air showers from Jan. 1989 to Oct. 1996. The variations are shown as the deviations from the average rate. The variations in the all air showers are smaller than 1%.

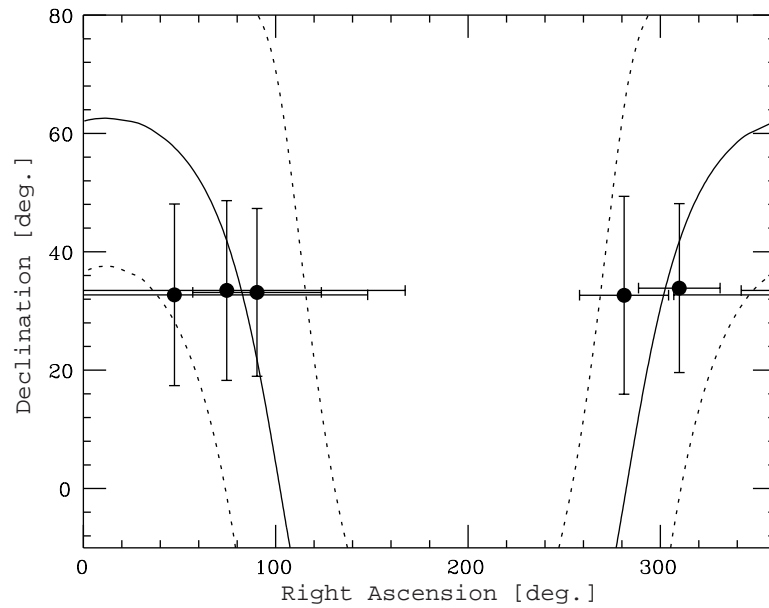


Fig. 19. - The directions of the clustered air showers in the ecliptic coordinate system. The solid and dashed curves show the galactic latitude at 0° and ±25°, respectively.

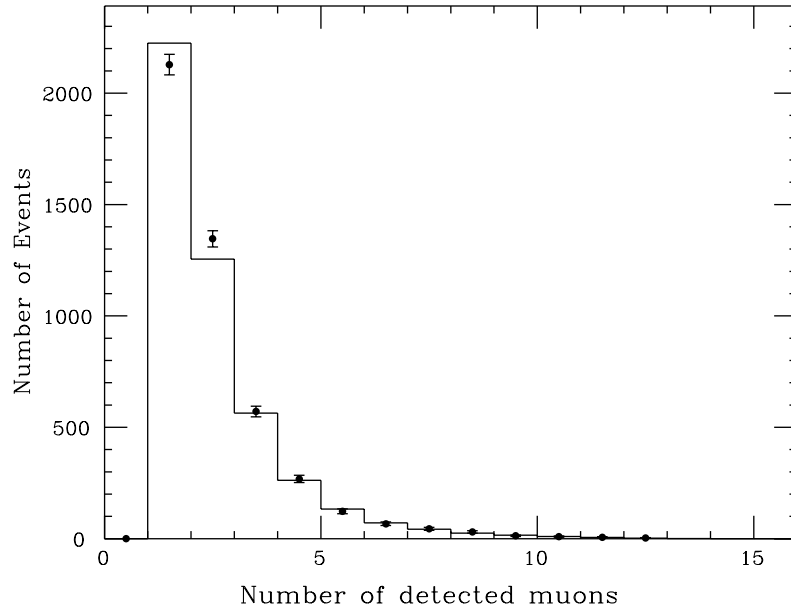


Fig. 20. – The number of detected muons per one shower. The air showers in clustered events are shown by the filled circles and the histogram shows the normal air shower events.

vational period for all sky in right ascension, however, was almost uniform; its variation from the average period is smaller than 1%. Also, the ordinary air showers have no such peaks. Figure 19 shows the average direction of each clustered event in the equatorial coordinate system. The solid and dashed curves show the galactic latitude 0° and $\pm 25^\circ$, respectively. All five clustered events are within the galactic latitude $\pm 25^\circ$. The chance probability of having five events within this region is 1.6%. This suggests that the clustered events appear to originate near to the galactic plane. Primary cosmic rays for the air showers observed in Mitsuishi are mostly protons. If the air shower was produced by a high-energy gamma ray, one expects that the number of observed muons in the shower should be small, compared with one produced by a proton. Figure 20 shows the number of muons per shower in the clustered events. There was no significant difference in the number of muons between the clustered events and the normal air shower events.

4. – Discussion and summary

We collected air shower data with a mean air shower size $N_e = 1.4 \times 10^5$ and with accompanying muon(s) of approximately $E_\mu \geq 6$ GeV, using the Mitsuishi air shower array over a period of eight years: from January 1989 to October 1996. The average event rate was approximately 1 event/min. Burst-like increases of air shower rates were searched for by grouping the events into clusters using a cluster method. If the expectation of occurrence for a cluster over the whole period (2427 days) is less than 0.05, we considered the cluster as significant. Five clustered events were found with a probability significantly different from expectation from a uniform distribution, the probability varying from 0.18×10^{-2} to 4.0×10^{-2} . The duration time of each cluster varied from 19.2 min to 40.0 hours. Size and zenith angles of the air showers in the clustered events have no

significant difference from the normal air showers. The arrival directions of the events are grouped in a region within the galactic latitude $\pm 25^\circ$. The chance probability of having five events within this region is 1.6%. This inclination of the arrival directions may suggest that their origins are in the nearby galactic arms. It is, however, improbable that the clustered events are initiated by charged particles (protons or heavy nuclei).

For a cosmic-ray proton of energy $\sim 10^{15}$ eV, its Larmor radius in the galactic magnetic field ($\sim 3\mu\text{G}$) is approximately 0.3 pc, which is much smaller than the size of the galactic arms. Consequently, charged particles coming from a galactic source a few kpc away suffer scattering in interstellar space, hence losing their original source directions. Similarly, the Larmor radius of heavy nuclei is much smaller than the size of the galactic arms, making it difficult to explain the origin of clustered events as heavy nuclei. On the other hand, if they are gamma-rays or neutral particles, scattering in the magnetic field should be negligible.

The EGRET experiment on CGRO reported an increase of delayed high-energy gamma-ray emission from a gamma-ray burst (GRB) in 1994. They detected very high-energy (200 MeV–10 GeV) photons for 1.6 hrs, following an intense burst on February 17, 1994 [14]. If the energy range of gamma-ray bursts extends to ultra high energy (UHE), presumably the air showers induced by the UHE gamma rays should accompany a small number of muons. Smith suggested a correlation of their cosmic-ray bursts with GRBs. We examined the number of detected muons per each shower in the clustered events, but found no difference in the number of muons between the clustered events and the normal air showers. If the clustered events include a significant number of air showers induced by UHE gamma rays from GRBs, one can expect that the arrival directions of the clustered air showers should have peaks in the directions of GRBs. There is no such peak in the distribution.

Another possible explanation for the clustering of the arrival directions is that they have heavier particles as their origins. The clustered events might be produced by the many secondary particles from some heavier primary particles, namely dusts, which are connected to the galactic arms. Berezhinsky, Hayakawa and Grindlay *et al.* [15-17] investigated the mechanisms for the propagation and destruction of relativistic dust grains in the interstellar medium. According to Grindlay's discussion, a relativistic grain in a certain size range can propagate for several hundred parsecs. Such a relativistic grain, when approaching the Earth, obtains a large electric charge as a result of interactions with solar photons. This increases the electrostatic forces, which break the grain. Because dust grains are abundant in the interstellar medium, they can be accelerated by the strong radiation pressure of supernova [18, 19] and/or by magnetic processes [20]. The clustered events could be produced by sub-relativistic secondaries from successive disintegrations of relativistic dust particles.

Evidence for dust-induced air showers was reported by Kitamura *et al.* [7]. They suggested that air showers showing chaotic behavior are possibly related to relativistic grains. We examined the clustered events for evidence of chaotic behavior using a fractal dimension analysis. No chaotic behavior was found in the clustered events. We also examined the time of occurrence of clustered events for correlation with Kitamura *et al.*'s chaotic air showers. No correlation was found. Non-random cosmic ray time series connected with the Galactic Arms appear to exist, but their origins are still mysterious.

* * *

We would like to thank Prof. T. KITAMURA of Kinki University for his valuable suggestions and many comments. We wish to thank Dr. J. HOLDER for correcting the English language in the manuscript. We also wish to thank the technical staff, K. HISAYASU, for the maintenance and the operation of the Mitsubishi air shower array.

REFERENCES

- [1] BHAT C. L. *et al.*, *Nature*, **288** (1980) 146.
- [2] BADINO G. *et al.*, *Lett. Nuovo Cimento*, **28** (1980) 93.
- [3] SMITH G. R. *et al.*, *Phys. Rev. D*, **28** (1983) 1601.
- [4] FEGAN D. J. *et al.*, *Proc. XVII ICRC (Paris)*, **16** (1981) 296.
- [5] SMITH G. R. *et al.*, *Phys. Rev. Lett.*, **50** (1983) 2110.
- [6] FEGAN D. J. *et al.*, *Phys. Rev. Lett.*, **51** (1983) 2341.
- [7] KITAMURA T. *et al.*, *Astropart. Phys.*, **6** (1997) 279.
- [8] KATAYOSE Y. *et al.*, *Proc. XXIV ICRC (Rome)*, **1** (1995) 301.
- [9] KAJINO F., PhD Thesis, Osaka City University (1981).
- [10] SATO T. *et al.*, *Proc. XIX ICRC (La Jolla)*, **8** (1985) 73.
- [11] KASAHARA K., *Proc. XXIV ICRC (Rome)*, **1** (1995) 399.
- [12] BUCCHERI R. *et al.*, *Data Analysis in Astronomy III*, edited by V. DI GESÙ, L. SCARSI, P. CRANE, J. H. FRIEDMAN, S. LEVIALDI, and M. C. MACCARONE (Plenum Press, New York) 1989, p. 67.
- [13] BUCCHERI R. *et al.*, *Astron. Astrophys.*, **201** (1988) 194.
- [14] HURLEY K. *et al.*, *Nature*, **372** (1994) 652.
- [15] BEREZINSKIY V. S. and PRILUTSKIY O. F., *Proc. XIII ICRC (Denver)*, **4** (1973) 2493.
- [16] HAYAKAWA S., *Astrophys. Space Sci.*, **16** (1972) 238.
- [17] GRINDLAY J. E. and FAZIO G. G., *Astrophys. J.*, **187** (1974) L93.
- [18] SPITZER L. jr., *Phys. Rev.*, **76** (1949) 583.
- [19] WOLFE B. *et al.*, *Phys. Rev.*, **79** (1950) 1020.
- [20] EPSTEIN R. I., *Mon. Not. R. Astron. Soc.*, **193** (1980) 723.